KEK Preprint 97-9
KOBE HEP 97-02
OULNS 97-01
TMU-HEP 97-21
April 1997
H

Measurement of the proton-antiproton pair production from two-photon collisions at TRISTAN

VENUS Collaboration

Abstract

The cross section of the $\gamma\gamma \to p\bar{p}$ reaction was measured at two-photon center-of-mass energy ($W_{\gamma\gamma}$) between 2.2 and 3.3 GeV, using the two-photon process at an $e^+ e^-$ collider, TRISTAN. The $W_{\gamma\gamma}$ dependence of the cross section integrated over a c.m. angular region of $|\cos\theta^*| < 0.6$ is in good agreement with the previous measurements and the theoretical prediction based on diquark model in the high $W_{\gamma\gamma}$ region.

(Submitted for publication)

** From April 1, 1997, **High Energy Accelerator Research Organization (KEK)** was newly established. The new organization is restructured of three reseach institutes, National Laboratory for High Energy Physics (KEK), Institues of Nuclear Study (INS), Univ. of Tokyo and Meson Science Laboratory, Faculty of Science, Univ. of Tokyo.*

High Energy Accelerator Research Organization (KEK), 1997

KEK Reports are available from:

Information Resources Division
High Energy Accelerator Research Organization (KEK)
1-1 Oho, Tsukuba-shi
Ibaraki-ken, 305
JAPAN

Phone: 0298-64-5137
Fax: 0298-64-4604
Cable: KEK OHO
E-mail: Library@kekvax.kek.jp (Internet Address)
Internet: http://www.kek.jp

Measurement of the proton-antiproton pair production from two-photon collisions at TRISTAN

VENUS Collaboration

H. Hamasaki [a], K. Abe [b], K. Amako [c], Y. Arai [c], Y. Asano [a], M. Chiba [d], Y. Chiba [e], M. Daigo [f], M. Fukawa [c,1], Y. Fukushima [c], J. Haba [g,2], H. Hanai [g], Y. Hemmi [h], M. Higuchi [i], T. Hirose [d], Y. Homma [j], N. Ishihara [c], Y. Iwata [k], J. Kanzaki [c], R. Kikuchi [h], T. Kondo [c], T. T. Korhonen [c,ℓ,3], H. Kurashige [h], E. K. Matsuda [m], T. Matsui [c], K. Miyake [h], S. Mori [a], Y. Nagashima [g], Y. Nakagawa [n,4], T. Nakamura [o,5], I. Nakano [p,6], S. Odaka [c], K. Ogawa [c,5], T. Ohama [c], T. Ohsugi [k], H. Ohyama [q], K. Okabe [m], A. Okamoto [h], A. Ono [r], J. Pennanen [c,ℓ], H. Sakamoto [h], M. Sakuda [c], M. Sato [i], N. Sato [c], M. Shioden [s], J. Shirai [c,7], T. Sumiyoshi [c], Y. Takada [a], F. Takasaki [c], M. Takita [g], N. Tamura [m,8], D. Tatsumi [g], K. Tobimatsu [t], T. Tsuboyama [c], S. Uehara [c], Y. Unno [c], T. Watanabe [u], Y. Watase [c], F. Yabuki [d], Y. Yamada [c], T. Yamagata [n], Y. Yonezawa [v], H. Yoshida [w] and K. Yusa [a]

[a] *Institute of Applied Physics, University of Tsukuba, Tsukuba 305, Japan*

[b] *Department of Physics, Tohoku University, Sendai 980, Japan*

[c] *KEK, National Laboratory for High Energy Physics, Tsukuba 305, Japan*

[d] *Department of Physics, Tokyo Metropolitan University, Hachioji 192-03, Japan*

[e] *Yasuda Women's Junior College, Hiroshima 731-01, Japan*

[f] *Faculty of Economics, Toyama University, Toyama 930, Japan*

[g] *Department of Physics, Osaka University, Toyonaka 560, Japan*

[h] *Department of Physics, Kyoto University, Kyoto 606, Japan*

[i] *Department of Applied Physics, Tohoku-Gakuin University, Tagajo 985, Japan*

[j] *Department of Electrical and Electronics Engineering, Kobe 657, Japan*

[k] *Department of Physics, Hiroshima University, Higashi-Hiroshima 724, Japan*

[ℓ] *Research Institute for High Energy Physics, Helsinki University, SF-00170 Helsinki, Finland*

[m] *Department of Physics, Okayama University, Okayama 700, Japan*

[n] *Division of Natural Sciences, International Christian University Mitaka 181 Japan*

[o] *Faculty of Engineering, Miyazaki University, Miyazaki 889-01, Japan*

[p] *Institute of Physics, University of Tsukuba, Tsukuba 305, Japan*

[q] *Hiroshima National College of Maritime Technology, Hiroshima 725-02, Japan*

[r] *Faculty of Cross-Cultural Studies, Kobe University, Tsurukabuto 1-2-1, Nada-ku, Kobe 657, Japan*

[s] *Department of Electronic and Computer Engineering, Ibaraki College of Technology, Hitachinaka 312, Japan*

[t] *Center for Information Science, Kogakuin University, Tokyo 163-91, Japan*

[u] *Department of Physics, Kogakuin University, Tokyo 192, Japan*

[v] *Tsukuba College of Technology, Tsukuba 305, Japan*

[w] *Naruto University of Education, Naruto 772, Japan*

[1] Present address: Naruto University of Education, Naruto 772, Japan.

[2] Present address: KEK, National Laboratory for High Energy Physics, Tsukuba 305, Japan.

[3] Present address: Accelerator Division, KEK, National Laboratory for High Energy Physics, Tsukuba 305, Japan.

[4] Present address: Faculty of Science, Ehime University, Matsuyama 790, Japan.

[5] Deceased.

[6] Present address: Department of Physics, Okayama University, Okayama 700, Japan.

[7] Present addrss: Bubble Chamber Physics Laboratory, Faculty Institute for Scientific, Tohoku University, Sendai 980-77, Japan.

[8] Present address: Department of Physics, Niigata University, Niigata 950-21, Japan.

1 Introduction

Since baryons are known to be composites of partons, *i.e.*, quarks and gluons, their production from the vacuum cannot be straightforward. The mechanism of the production is not well understood, despite that they are the fundamental elements forming the matter of the universe.

The pair production of a proton and an antiproton in two photon collisions,

$$\gamma\gamma \to p\bar{p}, \tag{1}$$

is one of the simplest processes suitable for investigating this problem. This reaction has been measured by many experiments at high-energy e^+e^- colliders [1–5], utilizing the two-photon process, *i.e.*, $e^+e^- \to e^+e^-p\bar{p}$, where the $p\bar{p}$ pair is produced from the collision of two nearly real photons emitted from incoming e^+ and e^-. The obtained experimental results, such as the production cross section, are consistent with each other among the experiments. However, we still have a large ambiguity due to limited statistics, especially in a high $\gamma\gamma$ center-of-mass energy region.

At low energies near threshold, reaction (1) must be complicated due to strong hadronic final-state interactions. The reaction is expected to show up its fundamental mechanism as the two-photon center-of-mass energy ($W_{\gamma\gamma}$) becomes larger, where a certain perturbative picture becomes applicable with helps from some customary phenomenology.

The cross section of reaction (1) has been estimated theoretically [6–8] on the basis of QCD, in the theoretical framework developed by Brodsky and Lepage [9]. The estimation depends on the model of the proton wave function. Among various ways of modeling, one of the most successful is the approach by Chernyak and Zhitnitsky [10] based on the QCD sum rule. Calculations based on their wave functions give reasonable estimates for other processes, such as $J/\psi \to p\bar{p}$ and magnetic form factors of the nucleons. However, the calculation for reaction (1) incorporating the same wave function [6] gives cross sections remarkably smaller than the experimental results, by one order of magnitude even at high energies around $W_{\gamma\gamma} = 3.0$ GeV.

Recently, a new calculation based on a diquark model has been proposed [11]. The model was found to reasonably reproduce the recent result from the CLEO group [5] in the high $W_{\gamma\gamma}$ region. Although the preference of the diquark model is apparent from the CLEO result, repeated measurements are necessary since the statistics is quite limited at high energies.

In this report, we present experimental results concerning the $\gamma\gamma \to p\bar{p}$

reaction in a $W_{\gamma\gamma}$ range between 2.2 and 3.3 GeV. The cross section was measured using the process $e^+e^- \to e^+e^-p\bar{p}$, at e^+e^- c.m. energies between 57 GeV and 64 GeV, by using the VENUS detector at the TRISTAN e^+e^- collider. The analyzed data correspond to an integrated luminosity of 331 pb^{-1}, at the luminosity-weighted average c.m. energy of 58 GeV. Although the integrated luminosity is about one forth of that of the CLEO measurement [5], the larger e^+e^- c.m. energies enable us to obtain comparable statistics in the high $W_{\gamma\gamma}$ region.

2 Experimental Apparatus

The VENUS detector is a general purpose magnetic spectrometer. Since the general description of the VENUS detector is given elsewhere [12], we briefly describe only those features relevant to the present analysis.

Charged particle tracks are detected by the central drift chamber (CDC) [13], placed in a 0.75 tesla axial magnetic field, produced by a superconducting solenoid. CDC is a cylindrical multi-wire drift chamber, having 29 sampling layers; 20 axial layers plus 9 stereo layers. Particles produced in a central region, $|\cos\theta| \leq 0.75$, are detected in all the layers, where θ denotes the polar angle from the beam axis. The momentum resolution is $\sigma_p/p = 0.8\% \times p_t(\mathrm{GeV}/c)$ for high momentum particles in the central region, where p_t is the transverse momentum with respect to the beam axis. For low momentum protons, in which we are interested in this analysis, the resolution is mainly determined by the multiple scattering in CDC. The typical value is 2.5% at $p_t = 0.5$ GeV/c. The energy loss in the detector materials is also significant for these protons. The average radial thickness of materials inserted between the interaction point and the first sampling point of CDC was 3.5 g cm^{-2}. The effect of the fluctuation of the energy loss is included in the above momentum resolution.

Flight times of charged particles were measured by the time-of-flight (TOF) counters [14]. The time resolution was 200 ps for isolated high-momentum tracks. The TOF counters were placed on the inner wall of the solenoid at a distance of 166 cm from the beam line, covering an angular range of $|\cos\theta| \leq 0.81$. The thickness of the materials between the outer wall of CDC and TOF was about 7.0 g cm^{-2}. The TOF counters provided signals for the event trigger as well.

Electromagnetic energies were measured by the barrel lead-glass calorimeter (LG) [15] and a pair of liquid-argon calorimeters (LA) [16]. LG covered a central region, $|\cos\theta| \leq 0.80$, and LA covered forward and backward regions, $0.79 \leq |\cos\theta| \leq 0.990$.

Although various event triggers were implemented for data acquisition, we used only those events triggered by the *coplanar* trigger in the present measurement. This trigger was issued when at least two tracks with an acoplanarity angle less than 25° were detected, where the acoplanarity angle is the supplement of the opening angle in the projection onto the plane perpendicular to the beam axis. The tracks were reconstructed from the CDC hit pattern by a fast track finding electronics (TF) [17], and required to be associated with TOF hits. The logic of TF with the TOF association was optimized for high-momentum tracks; the efficiency was about 97% for tracks with $p_t \geq 0.60$ GeV/c. However, the efficiency did not show a sharp cut-off at lower momenta, and an appreciable efficiency (about 50%) was kept for tracks with $p_t \sim 0.45$ GeV/c.

3 Event Selection

Because we are interested in the production of a $p\bar{p}$ pair from the collisions of nearly real photons, we selected so-called no-tag events, in which the recoiled e^+ and e^- escaped from the detection into small angles. From events triggered by the *coplanar* mode, we selected such events that consisted of exactly two oppositely charged tracks, with no other tracks coming from the neighborhood of the collision point. Tracks were counted if they were from a narrow cylindrical region around the interaction point, 1 cm in radius and $\pm$ 10 cm along the beam direction (z axis), and satisfied the conditions, $|\cos\theta| < 0.8$ and $p_t > 0.2$ GeV/c. For these events, the momenta of the two tracks were required to be within a region of $p_t > 0.45$ GeV/c and $p < 1.5$ GeV/c. The lower limit was set to ensure a substantial efficiency in the event trigger, while the upper limit was to preserve a good K/p separation by the flight-time measurement. For these two-track events, we required that the difference between the measured flight times of the two tracks should be smaller than 5 ns, and the observed total energy in LG and LA be smaller than 5.0 GeV.

The two tracks were required to be identified as a proton and an antiproton, where the difference between the measured flight time and that expected from the momentum and the path length was required to be within three standard deviations. The proton mass was assumed to give the expectation. The standard deviation was evaluated from the quadratic sum of the errors of the used quantities. The typical value was 250 ps. In addition, in order to reduce the contamination from pions and kaons in a high momentum region, the mass estimated from the TOF measurement was required to be within 0.1 GeV/c^2 from the proton mass. Figure 1 shows the correlation between the estimated masses of the two tracks, for the sample before the identification. The $p\bar{p}$ events are clearly separated from other combinations of the particles, such as $\pi^+\pi^-$, K^+K^-, $p\pi$ and so on.

Finally, the vector sum of p_t of the proton and antiproton (p_t-imbalance) was required to be smaller than 0.2 GeV/c. This cut was applied to reject non-exclusive $p\bar{p}$ events, and to restrict the virtuality of the colliding photons. A total of 311 events remained after the selection.

The candidate events was divided into two-dimensional bins of $W_{\gamma\gamma}$ and $\cos\theta^*$, with a width of 0.1 GeV for $W_{\gamma\gamma} < 2.75$ GeV and 0.1 for $|\cos\theta^*|$. Some wider $W_{\gamma\gamma}$ bins were used at $W_{\gamma\gamma} > 2.75$ GeV. The two-photon c.m. energy, $W_{\gamma\gamma}$, was calculated from the momenta of the proton and the antiproton after the correction for the energy loss in the materials. We used the angle between the proton momentum and the electron beam direction in the photon-photon c.m. frame to be the scattering angle θ^* with a good approximation.

4 Detection Efficiency

The detection efficiency was estimated by using a Monte Carlo (MC) event generator [18], based on an equivalent photon approximation (EPA) with the formula in [19]. Events were generated with a uniform $|\cos\theta^*|$ distribution. They were passed through a detector simulation including a trigger simulation, and the event selection. The efficiency was estimated in each $|\cos\theta^*|$-$W_{\gamma\gamma}$ bin. The interactions of the particles in the detector materials (multiple Coulomb scattering, energy loss and nuclear interactions) were simulated in the detector simulation. While the former two interactions are rather trivial, the nuclear interactions are expected to be much more complicated. We adopted a simplified model for these interactions, and optimized it by using information from real data. The interactions in the materials at small radii, were studied by investigating the properties, such as the vertex distribution, of low momentum tracks in multihadronic events. Further information, mainly concerning the large angle scattering and absorption in the materials at larger radii was obtained from the studies of the LG response for the selected $p\bar{p}$ events.

From the simulation, the detection efficiency was estimated to be maximum, about 10%, at $W_{\gamma\gamma}$ around 2.6 GeV in the angular region of $|\cos\theta^*| \leq 0.3$. The efficiency gradually decreases in larger $|\cos\theta^*|$ bins, due to the limited angular acceptance at each $W_{\gamma\gamma}$. The fall-off at smaller $W_{\gamma\gamma}$ is mainly determined by the track-finding efficiency in the event trigger. The efficiency at large energies, $W_{\gamma\gamma} > 2.7$ GeV, is limited by the particle identification efficiency. The estimated efficiency is about 2.5% in the largest $W_{\gamma\gamma}$ bin, $3.25 < W_{\gamma\gamma} < 3.35$ GeV, at $|\cos\theta^*| < 0.3$. The large-angle nuclear scattering and the absorption of antiprotons are also significant. About 30% of the events were estimated to be lost by these interactions.

The systematic error of the efficiency was estimated from ambiguities in the dominant source of the inefficiency. The uncertainty in the TF efficiency, which was estimated by comparing the response of TF to low-energy multi-track events with the simulation, corresponds to an efficiency error of 5% at $W_{\gamma\gamma}$ =2.2 GeV. Among the uncertainties in the nuclear interaction simulation, the largest is expected to be the uncertainty in the antiproton absorption. The corresponding efficiency error was estimated by comparing the simulation results with those from another hadronic interaction simulation program, FLUKA [20], to be 7% in all bins. The uncertainty from the particle identification was studied by varying the identification criteria. The corresponding error in the detection efficiency was found to be 10% at $W_{\gamma\gamma} = 2.7$ GeV, and to increase up to 14% at 3.05 GeV.

5 Background

Major sources of the background are expected to be the particle misidentification, and the contamination from non-exclusive processes such as $e^+e^- \to e^+e^-p\bar{p}\pi^+\pi^-$.

Concerning the misidentification background, the largest contribution comes from those events consisting of a proton and a negatively charged particle misidentified as an antiproton (pX^-). These are mainly produced by beam-gas and beam-wall interactions. The contamination was estimated to be (3 $\pm$ 3)% in all the $W_{\gamma\gamma}$ bins, from the z-vertex distribution of $p\bar{p}$ candidates selected with a looser z-vertex cut.

Events from meson-pair production, $\gamma\gamma \to \pi^+\pi^-$ and $\gamma\gamma \to K^+K^-$, can contaminate if both tracks are misidentified. The contamination was estimated to be (2 $\pm$ 2)% in the high energy region, $W_{\gamma\gamma} > 2.9$ GeV, by extrapolating the measured mass distribution of identified meson pair events into the proton mass region.

The contamination of events from non-exclusive processes, $\gamma\gamma \to p\bar{p} + X$'s in which X's were undetected, was estimated in each $W_{\gamma\gamma}$ bin, by comparing the p_t-imbalance distribution of the data with the simulation of the $\gamma\gamma \to p\bar{p}$ and $\gamma\gamma \to p\bar{p} + X$'s reactions.

The reaction, $\gamma\gamma \to p\bar{p}+X$'s, was simulated by using PYTHIA 5.7 [21]. The normalization of these MC processes was so determined that the sum of the two simulations fits the observed p_t-imbalance distribution as shown in Fig. 2. This figure shows the sum of the fit results. In this fit, the $W_{\gamma\gamma}$ bins above 2.6 GeV were combined because the statistics was small and the background dose not have steep $W_{\gamma\gamma}$ dependence in this region. The best fit, illustrated

with the histogram, well reproduces the observation, even in the large p_t-imbalance region above the cut. From the fit results, the contamination of the non-exclusive events was estimated to be $(8 \pm 3)\%$ on the average. Note that the contamination from non-exclusive events in which either proton or antiproton is misidentified is also included in this estimation, although their contribution is negligibly small.

6 Results and Discussions

The obtained event distribution was converted to the $\gamma\gamma \to p\bar{p}$ differential cross section, $\mathrm{d}\sigma(W_{\gamma\gamma}, |\cos\theta^*|)/\mathrm{d}|\cos\theta^*|$, by using the two-photon luminosity function [22] based on the EPA formula in [19]. The uncertainty in the luminosity function, due to the variation of the EPA formula, was estimated by comparing the used function with those derived from other formulas, and also with that from the exact QED calculation of the two-photon processes [18]. The uncertainty was found to be a few percent at maximum, and can be neglected safely. We included the form factor effect in the luminosity function for the suppression of the virtual-photon contribution, in which the ρ-meson mass was used as the mass scale [23]. It should be noted that the ambiguity in the effect of the photon virtuality, which is sometimes a serious problem in two-photon processes, is not appreciable in the present measurement. We observed only a few percent change in the cross section result when we removed the ρ-meson mass in the form factor for the test, although the CLEO group claimed that the ambiguity due to the choice of the form factor amounted to a 30% error [5]. The change in the form factor effected the luminosity function substantially. However, it also changed the efficiency, and then the net effects in the cross section were canceled. This is because the p_t-balance cut applied in the event selection tightly restricts the contribution of highly-virtual photons.

The measured differential cross section was summed over the whole angular coverage, $|\cos\theta^*| < 0.6$, in order to examine the $W_{\gamma\gamma}$ dependence. The obtained cross section, $\sigma(W_{\gamma\gamma})_{|\cos\theta^*|<0.6}$, is tabulated in Table 1 and plotted in Fig. 3. The previous measurements [3–5] are also shown in the figure, together with theoretical predictions [6,11,24]. Though the present measurement is somewhat larger than the previous measurements by CLEO [5] and ARGUS [4] at low energies, it is in good agreement with the CLEO measurement in the high energy region, $W_{\gamma\gamma} > 2.6$ GeV, with a comparable statistics. The preference of the diquark model is obvious from this result, at least in the high energy region.

In addition, a new theoretical prediction by Terazawa [24] which is expected to be valid near threshold, is shown in Fig. 3. The prediction reasonably reproduces the high-statistics measurement by CLEO at very low energies. This

fact may give us another knowledge on this process.

In order to proceed further investigation, the differential cross section was summed in the low energy region, $2.15 < W_{\gamma\gamma} < 2.55$ GeV, and in the high energy region, $2.55 < W_{\gamma\gamma} < 3.05$ GeV, separately. The obtained differential cross sections are compared in Fig. 4. We can see a distinctive difference between the two distributions; the cross section exhibits an enhancement at large angles in the low energy region, whereas it seems to be forward-peaking at high energies. The angular dependence in the high energy region is consistent with the prediction of the diquark model, as has been observed by the CLEO group [5]. However, looking at the result closely, the forward-peaking behavior of the diquark model seems to be insufficient to fully reproduce the measurement. The same tendency can be seen in the CLEO result, as well. This may suggest a need of other theoretical models. In any case, this fact indicates that there is a transition of the production mechanism around $W_{\gamma\gamma}$ = 2.55 GeV. The result suggests that a proton pair is mainly produced by the interaction of photons with a diquark in the high $W_{\gamma\gamma}$ region. This description fails to explain the angular distribution at low $W_{\gamma\gamma}$ regions, where a proton seems to be produced as a whole particle having a structure with small orbital angular momenta.

The distinction of the two mechanisms can be enhanced by using the difference in the angular dependence. The differential cross section was summed in a large-angle region, $|\cos\theta^*| < 0.3$, and in a region, $0.3 < |\cos\theta^*| < 0.6$, separately. The obtained cross sections are compared in Fig. 5. We can see that the large-angle cross section shows a steep fall-off at high energies, whereas the fall-off of the small-angle cross section is moderate. The difference is distinctive, and the latter overwhelms the former above $W_{\gamma\gamma} = 2.6$ GeV.

7 Conclusion

We have measured the cross section for the reaction, $\gamma\gamma \to p\bar{p}$, by detecting a two-photon collision reaction, $e^+e^- \to e^+e^-p\bar{p}$, at the e^+e^- c.m. energy around 58 GeV. The experiment was done by using the VENUS detector at the TRISTAN e^+e^- collider of KEK. From 331 pb^{-1} data, we have obtained the cross section in the two-photon c.m. energy range ($W_{\gamma\gamma}$) between 2.2 and 3.3 GeV, within the angular range of $|\cos\theta^*| < 0.6$. The precision of the result is comparable with the high-statistics measurement by CLEO group [5] in the high energy region, $W_{\gamma\gamma} > 2.6$ GeV.

The obtained cross section is consistent with those from the previous measurements. The enhancement at small angles in the high energy region, $W_{\gamma\gamma} >$ 2.6 GeV, which was shown in the CLEO measurement, has been clearly ob-

served. The preference of the diquark model [11] at high energies has been confirmed by the present results. Although it is not conclusive due to a poor statistics, there may be a hint that the predicted enhancement at small angles is not large enough to reproduce the measured results. More data are needed to proceed further discussion.

Acknowledgement

We would like to thank TRISTAN accelerator crew for their excellent operation of the accelerator. We acknowledge the outstanding support of the staff at KEK who enabled us to take data continuously. Thanks also go to the technical staff of the collaborating institutes.

References

[1] TASSO Collab., M. Althoff *et al.*, Phys. Lett. **130B**, (1983) 449.

[2] JADE Collab., W. Bartel *et al.*, Phys. Lett. **174B**, (1986) 350.

[3] TPC/2γ Collab., A. Aihara *et al.*, Phys. Rev. **D36**, (1987) 3506.

[4] ARGUS Collab., H. Albrecht *et al.*, Z. Phys. **C42**, (1989) 543.

[5] CLEO Collab., M. Artuso *et al.*, Phys. Rev. **D50**, (1994) 5484.

[6] R. Farrar *et al.*, Nucl. Phys. **B259**, (1985) 702; **B263**, (1986) 746(E).

[7] D. Millers and J. F. Gunion, Phys. Rev. D **34**, (1986) 2657.

[8] T. Hyer, Phys. Rev. D **47**, (1993) 3875.

[9] G. P. Leparge and S. J. Brodsky, Phys. Rev. D **22**, (1980) 2157.

[10] V. L. Chernyak and I. R. Zhitnitsky, Nucl. Phys. **B246**, (1984) 52.

[11] P. Kroll *et al.*, Phys. Lett. B **316**, (1993) 546.

[12] VENUS Collab., K. Abe *et al.*, J. Phys. Soc. Jpn. **561**, (1987) 3763.

[13] R. Arai *et al.*, Nucl. Instr. Meth. **A217**, (1983) 181.

[14] Y. Hemmi *et al.* , Jpn. J. Appl. Phys. **26**, (1987) 982.

[15] K. Ogawa *et al.*, Nucl. Instr. Meth. **A243**, (1986) 58;
T. Sumiyoshi *et al.*, Nucl. Instr. Meth. **A271**, (1988) 432.

[16] Y. Fukushima *et al.*, IEEE Trans. Nucl. Sci. **NS-36**, (1989) 670.

[17] T. Ohsugi *et al.*, Nucl. Instrum. Methods **A269**, (1988) 522;
Y. Arai and S. Uehara, Nucl. Instrum. Methods **A301**, (1991) 497.

[18] S. Uehara, KEK Report 96-11 (July 1996), unpublished.

[19] Ch. Berger and W. Wagner, Phys. Rep. **146**, (1987) 1.

[20] P. A. Aarnio *et al.*, Fluka user's guide. Technical Report TIS-RP-190, CERN, 1987, 1990.

[21] T. Sjöstrand, Cern-TH.7112/93 (1994).

[22] V. M. Budnev *et al.*, Phys. Rep. **15**, (1974) 182.

[23] M. Poppe, Intern. J. Mod. Phys. **A1**, (1986) 545.

[24] H. Terazawa, Institute for Nuclear Study, University of Tokyo, Report No. INS-Rep.-1122(1995).

Table 1
Measured cross section for $|\cos\theta^*| < 0.6$ as a function of $W_{\gamma\gamma}$. The first error is statistical and the second is systematic.

$W_{\gamma\gamma}$(GeV)	$\sigma(\gamma\gamma \to p\bar{p})$ (nb)
2.2	$7.56 \pm 1.71 \pm 0.70$
2.3	$5.01 \pm 0.65 \pm 0.43$
2.4	$2.90 \pm 0.41 \pm 0.26$
2.5	$0.89 \pm 0.17 \pm 0.12$
2.6	$0.96 \pm 0.21 \pm 0.15$
2.7	$0.23 \pm 0.09 \pm 0.04$
2.85	$0.22 \pm 0.08 \pm 0.04$
3.05	$0.10 \pm 0.07 \pm 0.02$
3.30	$0.10 \pm 0.10 \pm 0.02$

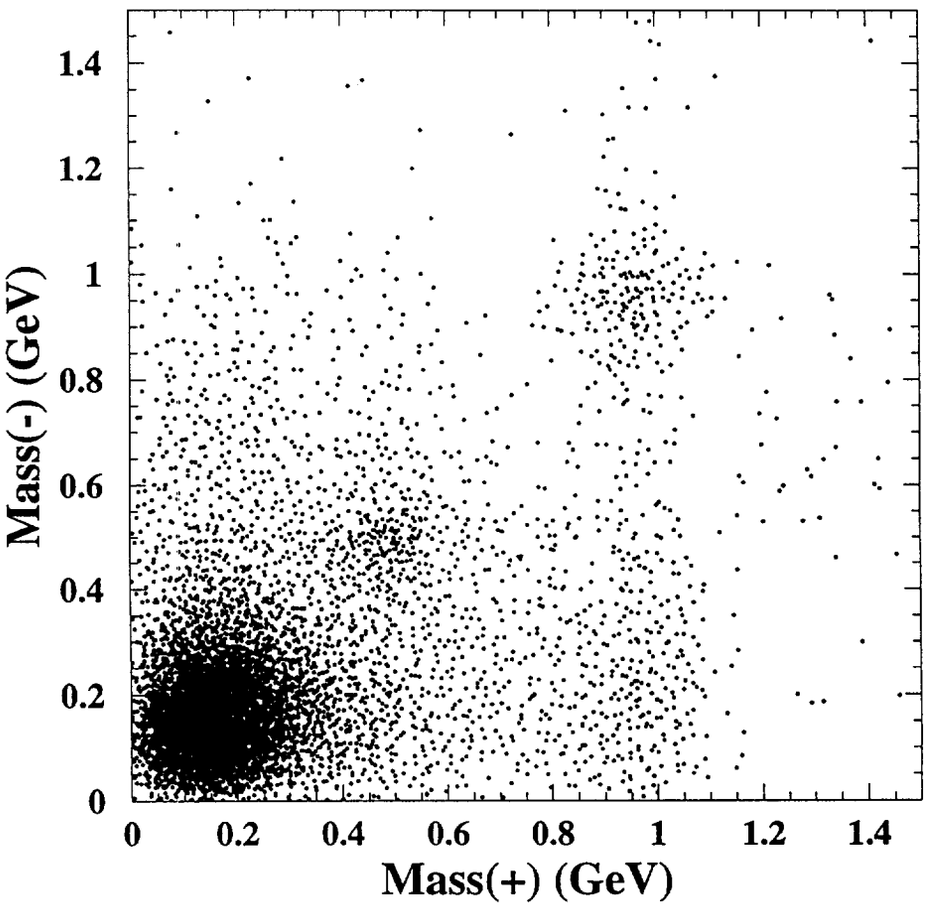

Fig. 1. Scatter plot of the masses calculated from the TOF for the positively(abscissa) and negatively(ordinate) charged particles in the event samples before the identification.

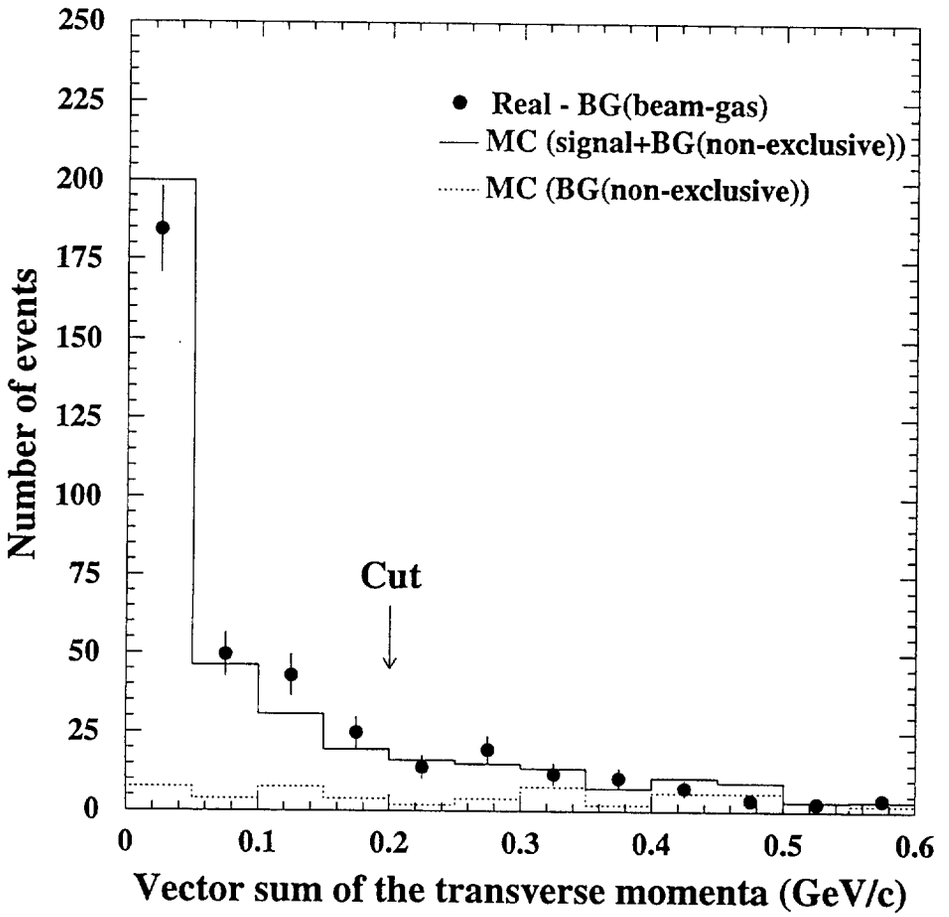

Fig. 2. $|\sum \vec{p}_t|$ distribution of the candidate events after the subtraction of the backgrounds from beam-gas/wall events. The dots with error bars are the experimental data, and the solid histogram is the sum of the MC data of $\gamma\gamma \to p\bar{p}$ and $\gamma\gamma \to p\bar{p}X$'s normalized by fitting the experimental data. The dashed histogram is the estimated contribution from $\gamma\gamma \to p\bar{p}X$'s.

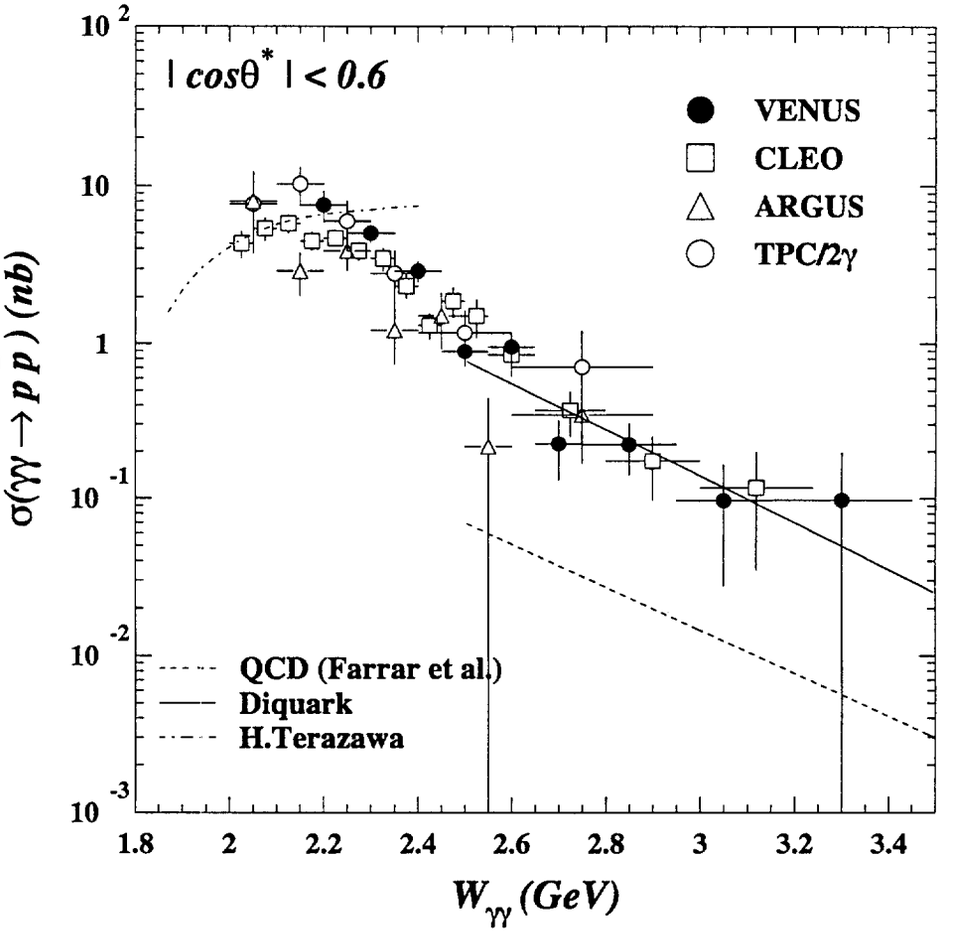

Fig. 3. Measured cross section for $\gamma\gamma \to p\bar{p}$. The present results (dots with error bars) are plotted together with those from the previous experiments [3–5]. The results from three theoretical calculations drawn by a dashed curve [6], a solid curve [11] and a dashed-dot curve [24] are also shown. The experimental and theoretical results are for the range of $|\cos\theta^*| < 0.6$. The error bars are statistical only.

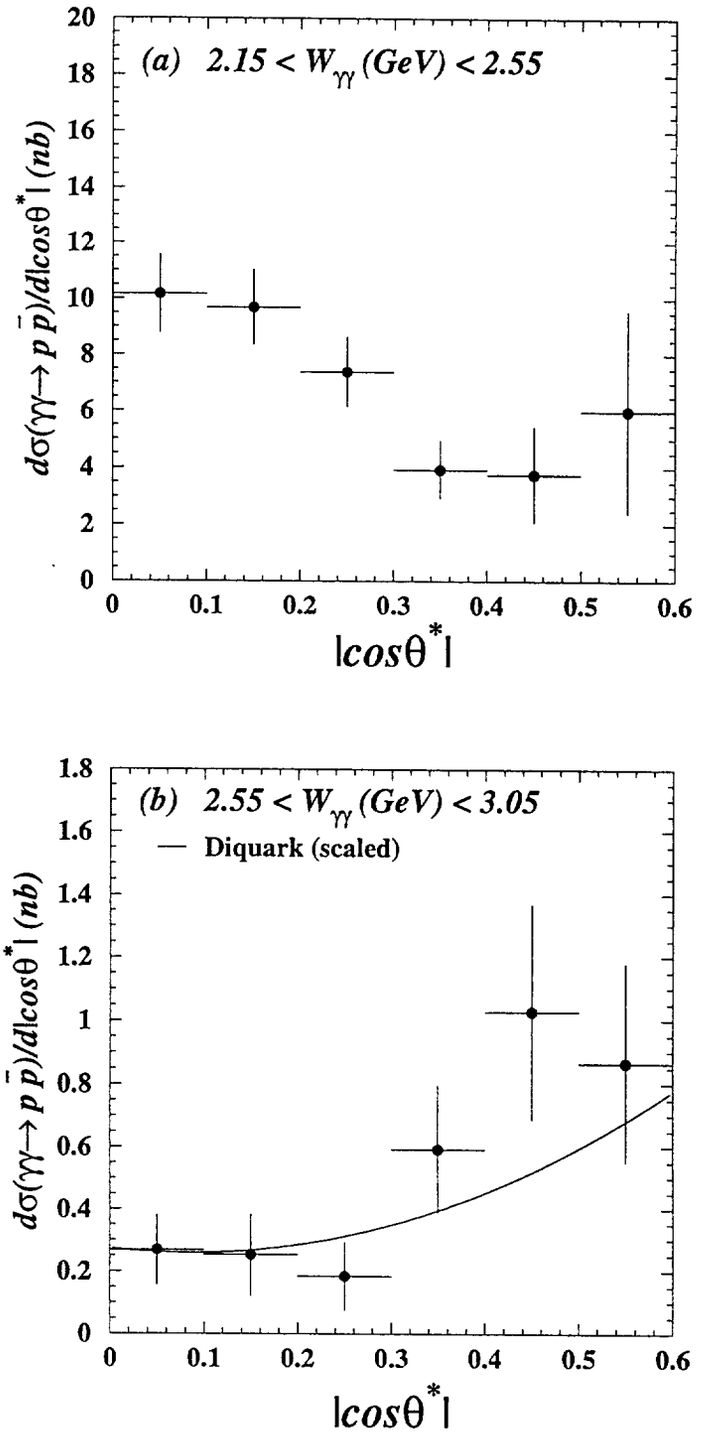

Fig. 4. Measured differential cross section for $\gamma\gamma \to p\bar{p}$: (a)2.15 < $W_{\gamma\gamma}$ < 2.55 GeV and (b)2.55 < $W_{\gamma\gamma}$ < 3.05 GeV. In (b), the calculation of a diquark model whose the normalization is scaled to agree with the measurement is also drawn. Errors are statistical only.

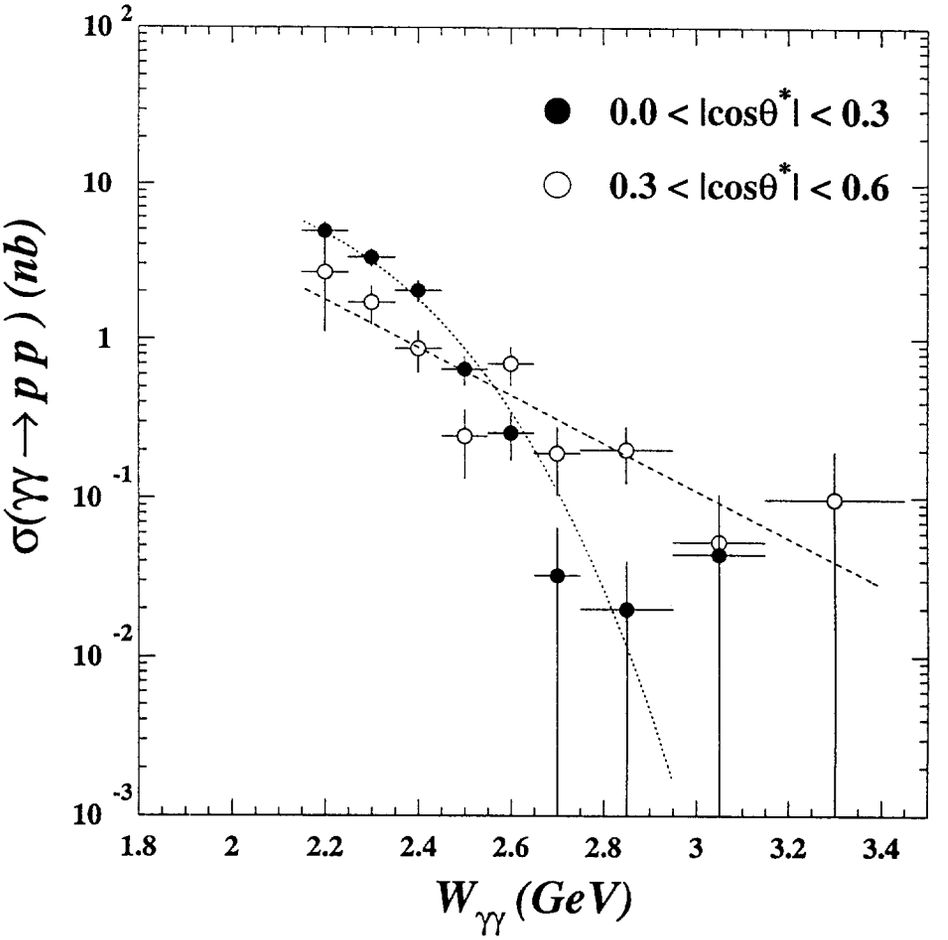

Fig. 5. The measured c.m. energy dependence of the cross section for the $|\cos\theta^*|$ ranges from 0.0 to 0.3 (open circles) and from 0.3 to 0.6 (closed circles). No event was found in the bin of $W_{\gamma\gamma} = 3.3$ GeV for $0.0 < |\cos\theta^*| < 0.3$ (This corresponded to the upper limit of the cross section 0.14 nb, with 90% confidence level). The lines are manually drawn to guide the eye.